An analysis of some replicated wind tunnel experiments on instantaneously released heavy gas clouds dispersing over solid and crenellated fences

J.K.W. Davies [a], D.J. Hall [b],[*]

[a] *Safety Engineering Laboratory, Health and Safety Executive, Broad Lane, Sheffield S3 7HQ, UK*
[b] *Building Research Establishment, Garston, Watford WD2 7JR, UK*

Abstract

The purpose of the work discussed here was to study the nature and extent of the disturbance to the dispersion process when a dense gas cloud originating from an instantaneous release and dispersing over level ground is obstructed by a fence. This information is needed to extend the scope of the HSE risk assessment tool RISKAT [1] to allow for the effects of methods of containment such as bunds and of pre-existing obstacles such as rows of buildings. Evidence is produced for a power-law relationship between the reduction in cloud concentration attributable to the presence of a solid fence and the fence height.

Keywords: Fence; Heavy gas cloud; Wind tunnel experiment

1. Introduction

The purpose of this work here was to study the nature and extent of the disturbance to the dispersion process when a dense gas cloud originating from an instantaneous release and dispersing over level ground is obstructed by a fence. This information is needed in order to extend the scope of the HSE risk assessment tool RISKAT [1] to allow for the effects of methods of containment such as bunds and of such obstacles such as rows of buildings.

---

[*] Corresponding author.

The experimental work which forms the basis of the present analysis was carried out by Hall et al. [2,3] at Warren Spring Laboratory under contract to HSE as part of the EC Major Technological Hazards Project BA "Research on continuous and instantaneous heavy gas clouds", which is described by Builtjes [4]. The analysis itself was carried out as part of HSE's contribution to the current EC Science and Technology for Environmental Protection project FLADIS "Research on the dispersion of two phase flashing releases", and falls into two parts, which are:

1. a comparison of dispersion behaviour over solid fences with that over unobstructed flat terrain, and
2. a comparison of dispersion behaviour over crenellated fences with that over solid fences.

Section 2 of the Report contains a brief description of the experimental set-up; Section 3 and Section 4, respectively, describe analyses of the effect of the fence and whether it is solid or crenellated. Finally, Section 5 discusses the findings and draws some conclusions.

2. The experimental set-up

The experiments using fences, described in [3], and the earlier experiments on flat terrain, described in [2], were designed as $1/100$ scale wind tunnel models of the Thorney Island field trials [5,8] and were intended to examine the natural variability in repeated, identical releases. The layout of the experiments is shown in Fig. 1. The source was a collapsing tent of 14 m diameter (full-scale dimensions only are given here and in what follows) and height $H = 13$ m, the sides of which were dropped suddenly to release a cylinder of gas as in the full-scale trials. Because the experiments required a large number of repeat measurements, which is a time consuming activity, gas concentration measurements were made at only a few stations and only a single fence position was used. Because of the need to model buoyancy effects at small scale, the experiment used relatively low windspeeds, ranging between 0.78 and 1.74 m s^{-1}. However, as was remarked in the original reports on the work, these were kept as high as practicably possible in order to minimise any possible Reynolds number effects.

The releases were monitored by two pairs of vertically mounted fast-response gas sensors, one pair in the near field, 70 m downwind of the source, and the other in the far field, 200 m downwind. The lower sensor in each pair was situated 0.4 m above ground, the lowest height used in the full-scale trials, and the upper sensor was at a height of 2.4 m, close to the upper edge of the cloud in the higher Richardson number releases. Both the distances and the heights employed in the wind tunnel experiments corresponded to values used in the full-scale trials. With no fence present, the maximum ground level concentration was expected to fall to about 10% by volume, expressed as a fraction of the source concentration, at approximately 70 m downwind and to about 2% by volume at approximately 200 m, a value close to the lower flammability limit of many flammable gases.

The fence was situated 100 m downwind of the source at right-angles to the wind tunnel centre-line, a position close enough to the near field sensors to enable any upwind
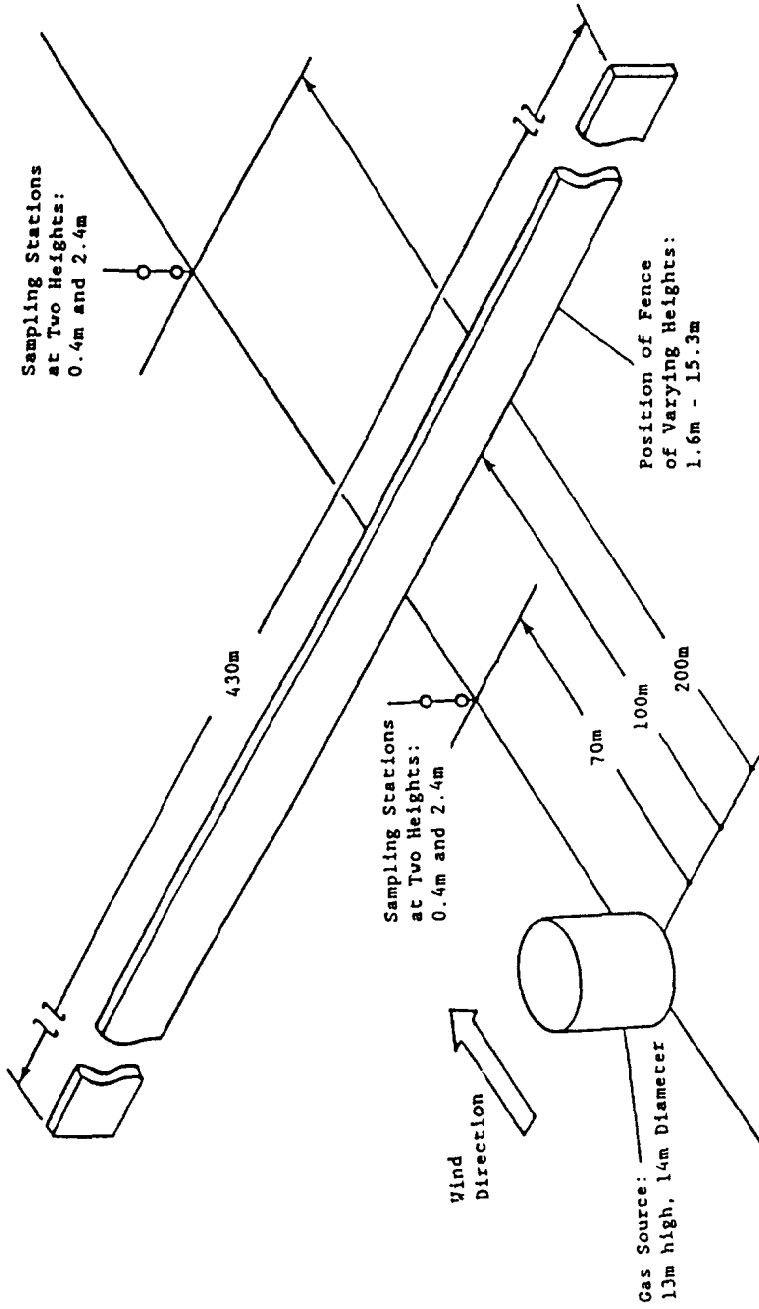
Fig. 1. The layout of the repeat-run wind tunnel experiments, with a solid fence in position.

Table 1
Richardson number/fence height (Ri/ h) combinations employed in the WSL solid fence (S) and crenellated fence (C) experimental runs

Ri	h (m)					
	1.6	3.8	5.1	7.6	10.2	15.3
0		C	S	S C	S	S C
1		S		S		S
2		S C		S C		S C
5		S		S		S
10	S	S C	S	S C	S	S C

"blocking" effect due to the fence on the gas cloud to be detected, and close enough to the far field sensors to ensure that they were in the flow separation region for high fences and in the flow re-attachment and recovery region for low fences. Two types of fence were employed, solid and crenellated, the crenellations being square elements giving 50% open area. The solid fences were intended to represent impermiable obstructions such as bunds, and the crenellated fences were intended to represent permiable obstacles such as a row of buildings. The choice of open area of the crenellated fence is to some extent arbitrary, as the whole range of open areas can occur readily in practical cases. 50% was used in the experiments for two reasons. Firstly, it is the approximate open area for porous fences which produces the lowest mean velocities and turbulence in the wake. Secondly, it matched a field experiment using a crenellated fence carried out as part of the same EC project [4]. Fence heights were varied in six
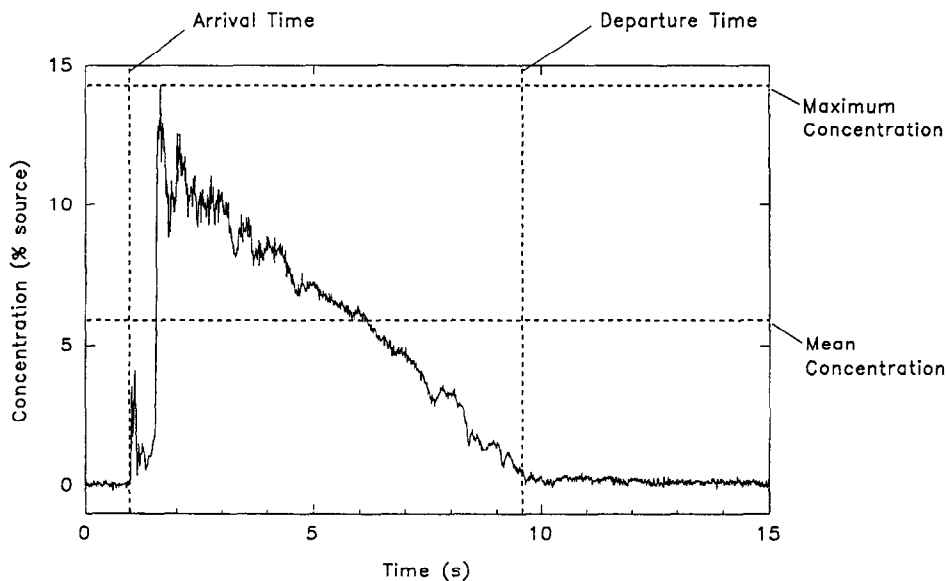

Fig. 2. A typical concentration/time trace from the experiments with the analysis parameters marked on it.

steps from $h = 1.6$ m to $h = 15.3$ m, i.e. from 10% of the source height to 20% more than the source height.

The main scaling parameter used in the wind tunnel modelling was the bulk Richardson number Ri, defined as where the characteristic length scale L is set equal to the height of the tent H. The windspeed U is at the tent height H. The Richardson numbers

$$\text{Ri} = g \frac{\rho_{gas} - \rho_{air}}{\rho_{air}} \frac{L}{U^2}$$

ranged from Ri = 0, neutral buoyancy, through Ri = 1 and 2, where gravity effects become significant compared with kinematic effects, to Ri = 5 and 10, where the release, at least in its early stages, is dominated by gravity-driven conditions. At the highest Richardson number, the release conditions approach those occurring in still air, but with a wind-driven drift of the cloud. The Thorney Island releases were mostly in the range Ri = 2 to Ri = 10.

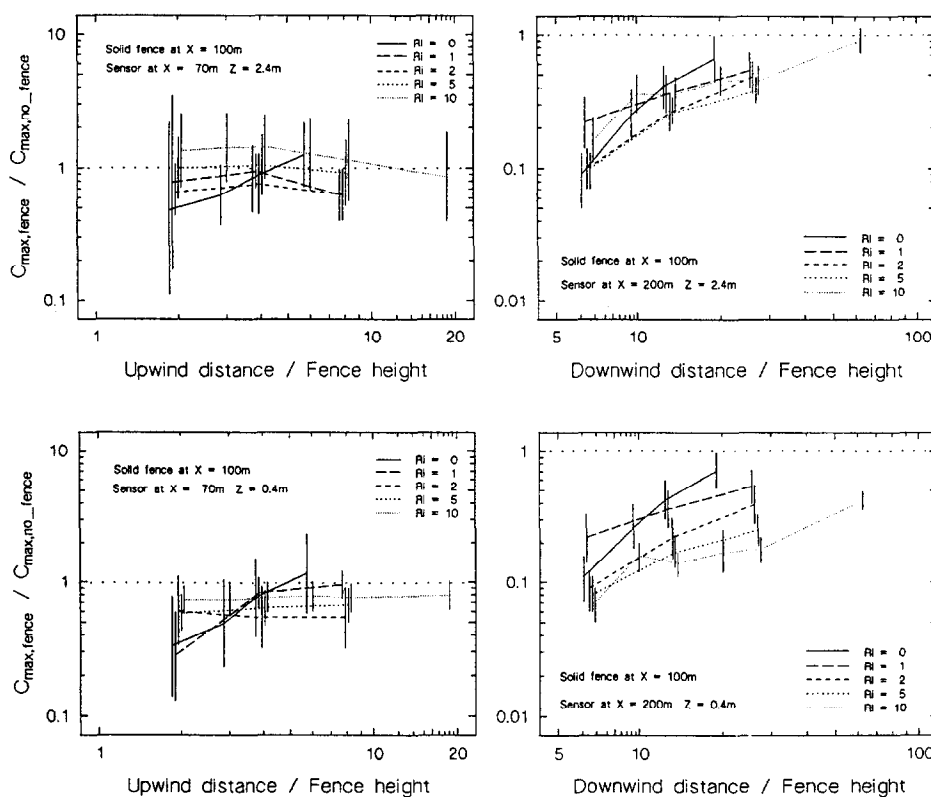Table 1 shows the combinations of Richardson number and fence height and type

Fig. 3. Variation of $C_{max,fence} / C_{max,no\ fence}$ with scaled distance from fence at the four sensor positions.

used in these experiments. Each experiment was replicated 50 times, a level of replication which, in the light of experience gained in the flat terrain runs (which used up to 100 repeats), was thought sufficient to enable statistical parameters to be determined accurately enough without imposing too great an experimental load. It may be shown [6] that for a sample of size n from a normal distribution the relative error in the determination of the standard deviation σ is $(2n)^{-1/2}$ as $n \to \infty$, so that for $n = 50$ one might expect a relative error of approximately 10%. As mentioned in the following section, the work described in [3,4] showed that the cloud parameters were generally log normally distributed, so that the log standard deviations derived from the replicated experiments were accurate to within 10%.

3. Analysis of the solid fence results

The data were numerically analysed in the original work to obtain values of a number of basic parameters associated with the gas clouds, and these are used in the analysis below. A full description of the procedures used can be found in [2], but, for
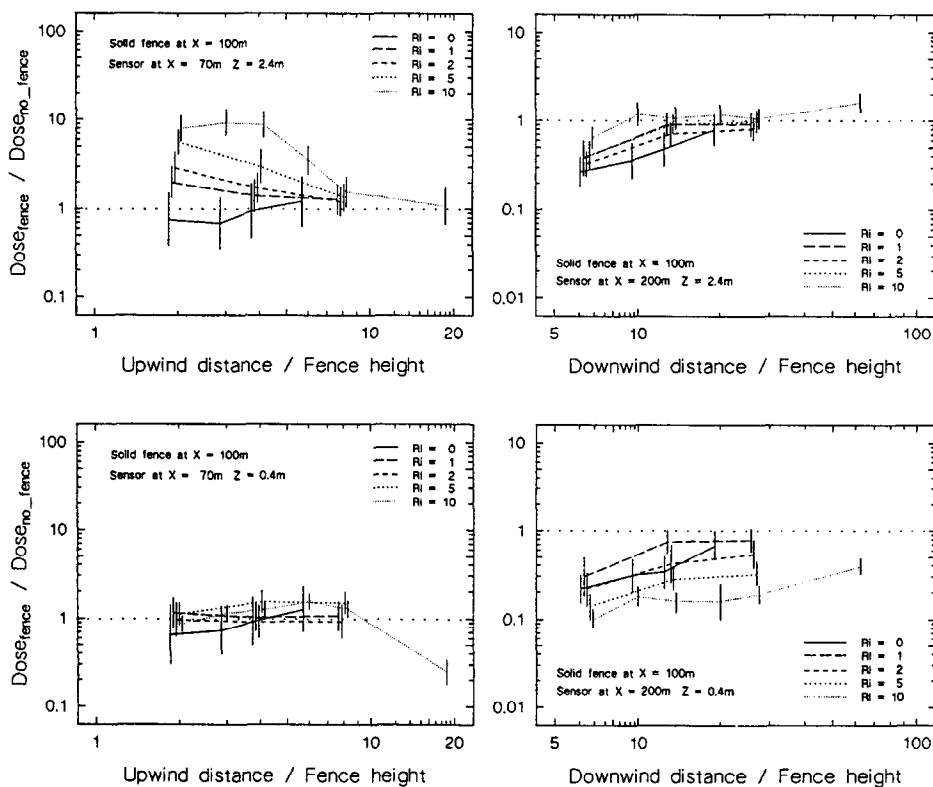

Fig. 4. Variation of dose$_{\text{fence}}$/dose$_{\text{no fence}}$ with scaled distance from fence at the four sensor positions.

convenience, the definitions used here are repeated below together with some brief comments. Fig. 2 shows an example of a concentration/time trace from a gas cloud with various parameters marked on it. Some of the parameters refer to the "noise level" of the concentration signal. This was the small level of perturbation recorded by the sensors when no gas was present, its RMS value being equivalent, typically, to $\approx 0.02\%$ of BCF, the gas of greatest density used in the experiments. In order to determine parameters where concentrations close to this level were important, a five point running average of the concentration was used and a "noise level" of this averaged concentration, high enough to avoid all residual perturbations, was set by examining some of the traces by eye. Values of the "noise level" set in this way were all between 0.05% and 0.15% of the source concentration, with the exception of the worst case, which was 0.4%.

The parameters determined in [2,3] were

(i) Maximum recorded concentration C_{max}.

(ii) Cloud arrival time T_{arr}: the earliest time at which the concentration rose above the set "noise level".
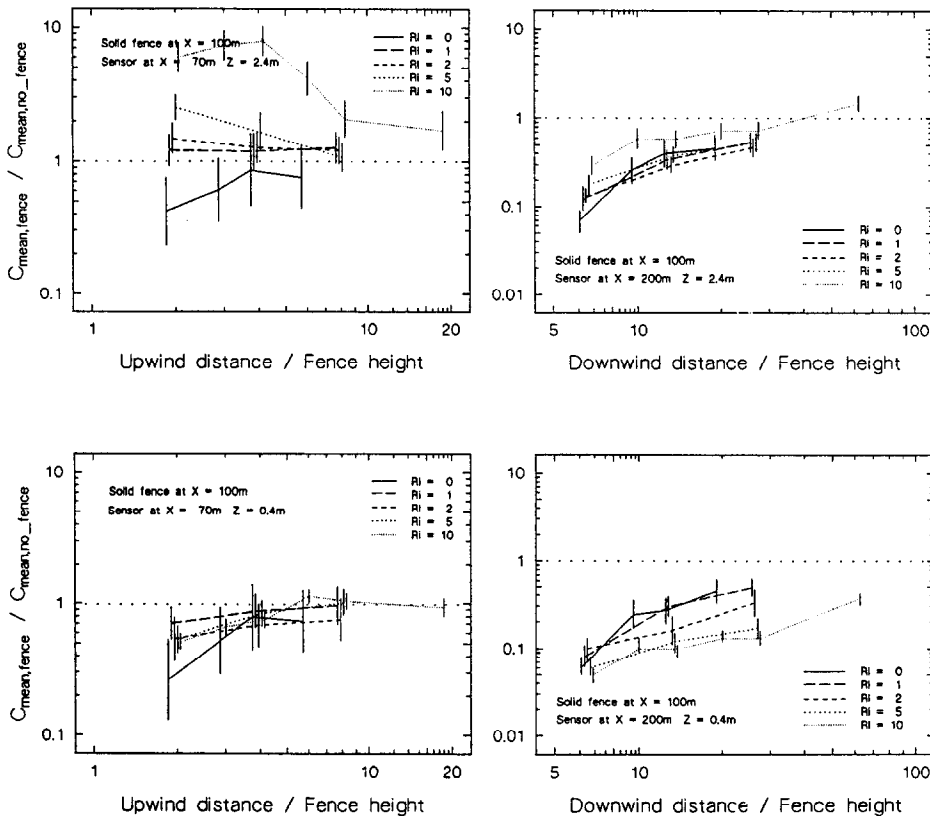

Fig. 5. Variation of $C_{mean,fence} / C_{mean,no\ fence}$ with scaled distance from fence at the four sensor positions.

(iii) Cloud departure time T_{dep}: the latest time at which the concentration fell below a set threshold (set a little above the general noise level of the sensor output) plus 3% of the maximum concentration. This was found by checking backwards along the trace to the first occurrence of this point. The concentration defining the "departure time" was set at this relatively high level to avoid picking up too much of the long "tail" of residual concentration which appeared in some of the traces, as this is to some extent caused by scale effects at the relatively low Reynolds numbers of the experiments.

(iv) Mean concentration C_{mean}: the averaged concentration between the cloud arrival and departure times.

In addition, two other parameters are used here, viz:

(i) cloud passage time T_{pass}: the difference between the cloud arrival and departure times;

(ii) dose: the product of C_{mean} and T_{pass}.

All the figures shown here, and the later ones for the crenellated fence results, follow the same general pattern, adopted here in order to present the large volume of data collected during the replicated experiments in a manageable form and in such a way as to aid in extending the scope of the HSE risk assessment tool RISKAT [1]. Each figure
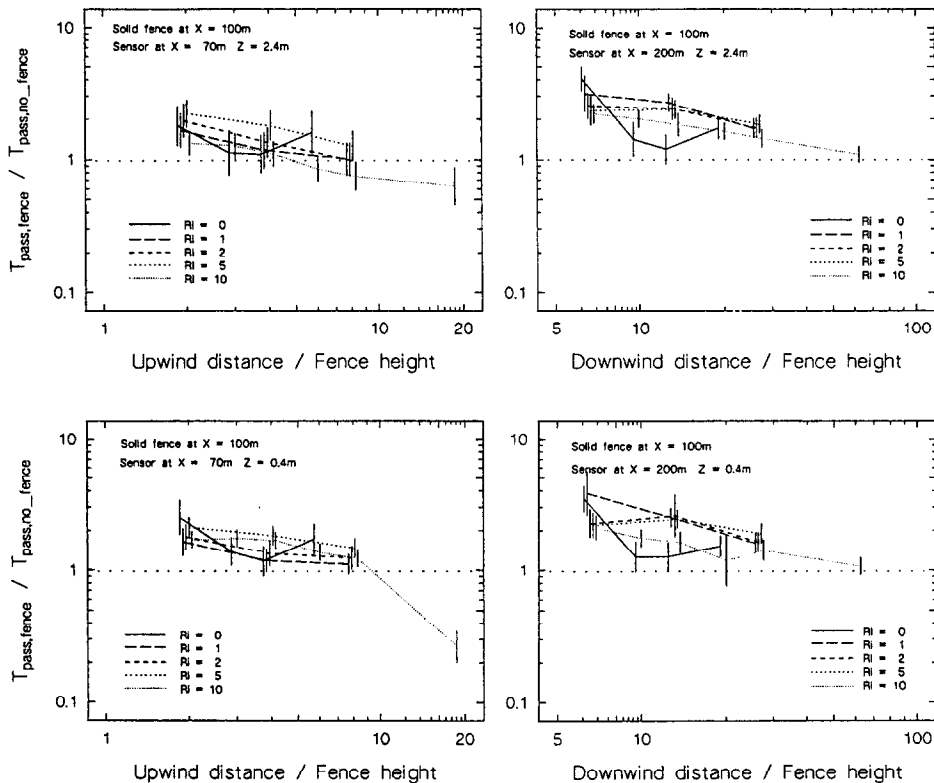
Fig. 6. Variation of $T_{pass,fence} / T_{pass,no\ fence}$ with scaled distance from fence at the four sensor positions.

incorporates all the relevant Richardson number/fence height cases listed in Table 1. The results for the near field and far field ground level sensors ($Z = 0.4$ m) are plotted in the lower left and lower right quadrants, respectively, and those for the near field and far field sensors at $Z = 2.4$ m are plotted in the upper left and upper right quadrants, respectively. The horizontal axes show distances upwind and downwind of the fence scaled by fence height. Scaling by fence height was adopted because it was hoped thereby to show the presence of effects due to blocking and flow retardation of the gas cloud upwind of the fence and to flow reattachment downwind of the fence. The vertical axes show the relevant parameter ratio, which is plotted in the form of an error bar. The central value of each error bar corresponds to the mean of the log ratio, and the upper and lower limits to the mean plus or minus one standard deviation. In the limited statistical analysis carried out in the original work [3,4], the variability in the parameters associated with the gas cloud were found to be generally log normally distributed. As the cloud parameters themselves are log normal, it follows that the cloud parameter ratios are also log normal, so that the log ratios are normal and the error bars show the 16th, 50th and 84th percentiles of the ratio. There is thus a 68% chance (roughly 2:1 in terms of odds) that any experimental realisation of the ratio—such as would be obtained
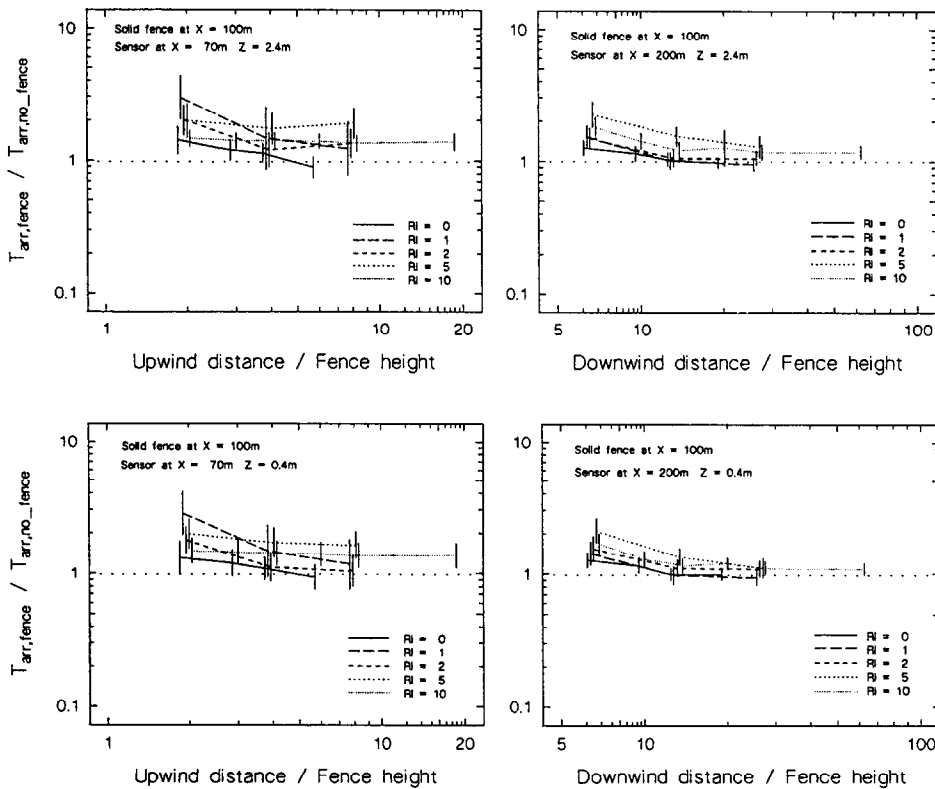

Fig. 7. Variation of $T_{arr,fence} / T_{arr,no\ fence}$ with scaled distance from fence at the four sensor positions.

by performing two runs under nominally identical conditions, one with the fence and the other without the fence—will be within the plotted limits.

Fig. 3Fig. 4Fig. 5Fig. 6Fig. 7Fig. 8 show results from the solid fence measurements. Fig. 3 shows measurements of maximum concentration C_{max}. These fall into two categories of behaviour: those derived from upwind measurements and those from downwind measurements. For the upwind sensors, it will be seen that for the neutrally buoyant and low Richardson number releases (Ri < 2), and particularly at the lower sampling station, there was a tendency for the C_{max} ratio to fall as fence height was increased or, equivalently, for the sensors to enter the flow retardation region which [7] extends a few fence heights upwind of the fence. The effect was not observed for high Richardson numbers. For the downwind sensors there was a tendency throughout the range of Richardson numbers considered, for all but the lowest fence, for the C_{max} ratio to reduce with increasing fence height, reaching a value of 0.1 for the highest fence employed. The effect became more pronounced as the Richardson number increased (particularly at ground level) and persisted up to at least 100 fence heights downwind, for Ri = 10, at ground level, and for approximately 70 fence heights at $Z = 2.4$ m. Similar behaviour was noted for the dose ratio in Fig. 4 and the C_{mean} ratio in Fig. 5,
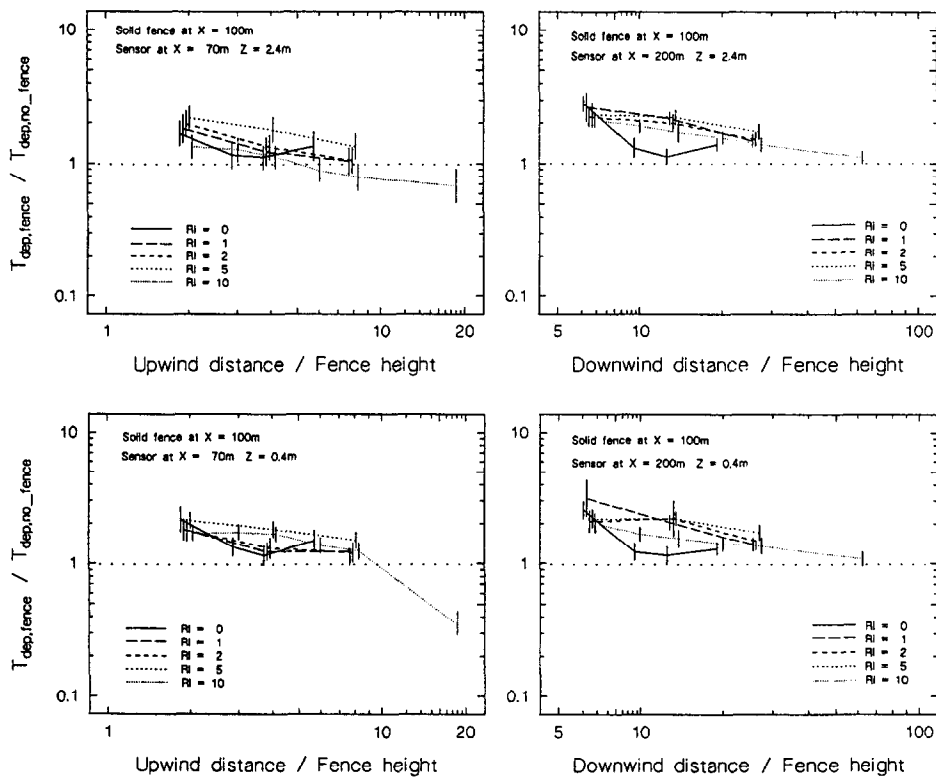

Fig. 8. Variation of $T_{dep,fence} / T_{dep,no\ fence}$ with scaled distance from fence at the four sensor positions.

Table 2
The median of the standard deviation of the log C_{max} ratio for the fence/no fence comparison, taken over all fence height/Richardson number combinations in each quadrant. The entry in parentheses is the corresponding 90th to 10th percentile ratio

	$X = 70$ m	$X = 200$ m
$Z = 2.4$ m	0.55 (4.1:1)	0.31 (2.2:1)
$Z = 0.4$ m	0.31 (2.2:1)	0.32 (2.3:1)

except that in these cases there was distinct evidence of upwind blocking by the fence of the passage of the gas cloud, judging from the steady increase of dose and C_{mean} with fence height and Richardson number at $Z = 2.4$ m. Also, the rate of decay of dose downwind of the fence was less pronounced than that of either C_{max} or C_{mean}; this is discussed further below.

The comparative behaviour of the time-based cloud parameters T_{pass}, T_{arr} and T_{dep} are
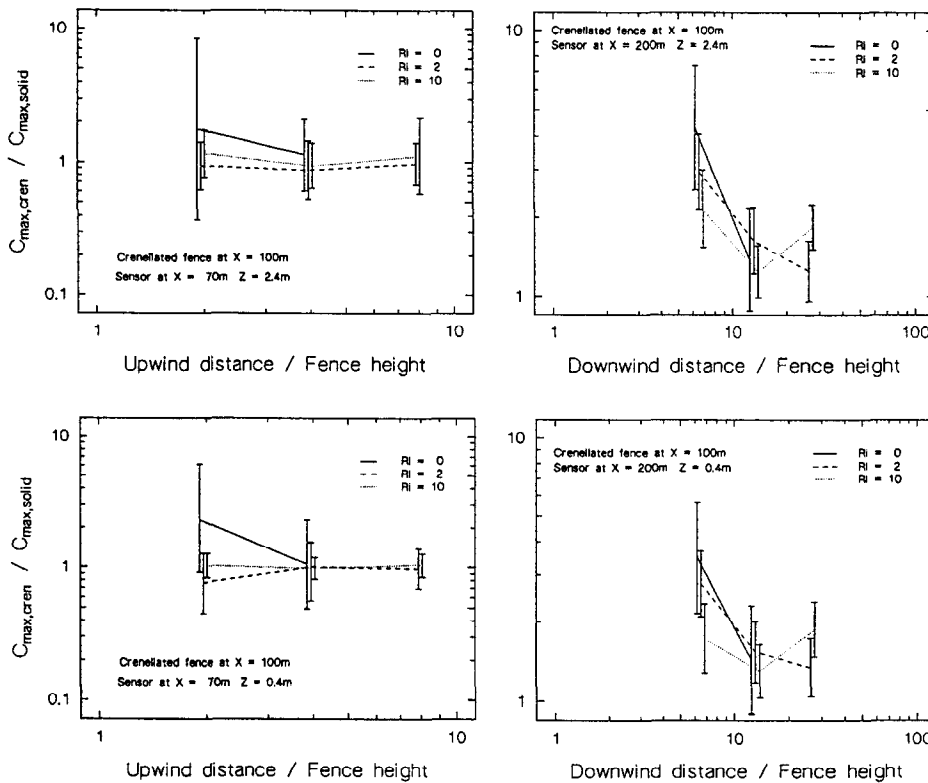

Fig. 9. Variation of $C_{max,cren} / C_{max,solid}$ with scaled distance from fence at the four sensor positions.

shown in Figs. 6–8, Fig. , respectively. As will be seen, in non-neutral conditions there is a general tendency for the parameter ratios to increase as fence height is increased, although the effect seems to reach its peak at $Ri = 5$ and to decline for the higher Richardson number. However, in neutral conditions the ratios for T_{pass} and T_{dep} show clear minima at approximately 3-4 fence heights upwind and 8-12 fence heights downwind. These locations correspond, respectively, to the start of the flow retardation region upwind of the fence and the start of the reattachment region of the separated flow downwind of the fence. The tendency for the T_{pass} ratio to increase with fence height, especially downwind of the fence, explains why the downwind decay of dose shown in Fig. 4 is less than the corresponding decay of C_{max} in Fig. 3 and C_{mean} in Fig. 5, since the dose is by definition the product of C_{mean} and T_{pass}.

So far as variability between releases is concerned, the effects of the solid fence are perhaps most clearly seen in the plots of the C_{max} ratio shown in Fig. 3. In general, variability as measured by the standard deviation of the log C_{max} ratio is greater for the highest upwind sensor, at $Z = 2.4$ m, than for the other three sensors, ranging from 0.15, for the downwind ground level sensor with a fence height of 1.6 m and $Ri = 10$, to 1.54
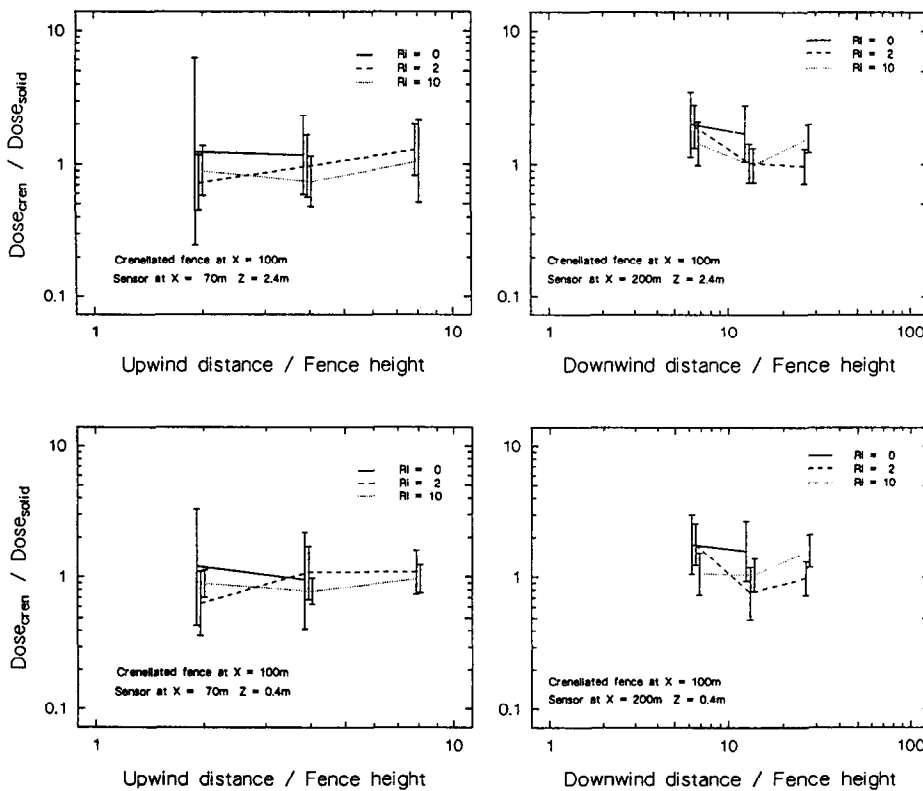

Fig. 10. Variation of $dose_{cren}/dose_{solid}$ with scaled distance from fence at the four sensor positions.

for the upwind sensor at $Z = 2.4$ m with a fence height of 15.3 m and $Ri = 0$. This implies that the ratio of the 90th to the 10th percentile (the "percentile ratio") ranges from 1.5:1 to 50:1, although generally the percentile ratio is less than 10:1. The median values over all fence height/Richardson number combinations in each quadrant are shown in Table 2. From the table it may be seen that for the ground level sensor downwind of the fence the ratio of the 90th to the 10th percentile of $C_{max,fence}/C_{max,no}$ $_{fence}$ is 2.3:1.

4. Analysis of the crenellated fence results

The crenellated fence/solid fence comparison plots are shown in Fig. 9Fig. 10Fig. 11Fig. 12Fig. 13Fig. 14. As will be seen from Table 1, the number of fence height/Richardson number combinations for which direct comparisons can be made is limited to eight cases in all, covering fence heights of $h = 3.8$, 7.6 and 15.3 m and
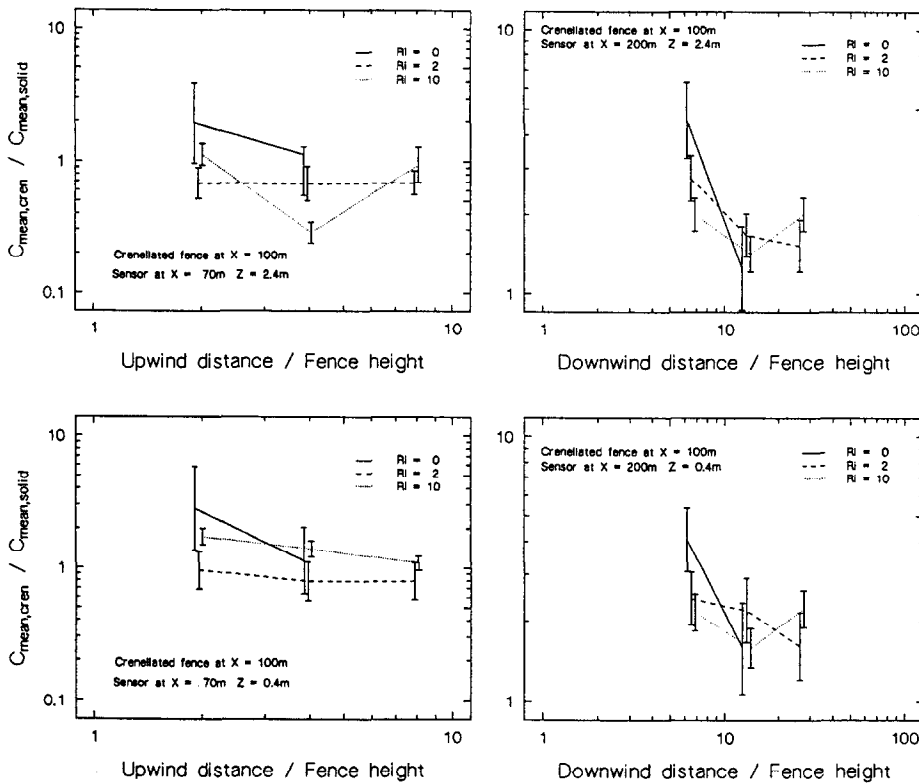

Fig. 11. Variation of $C_{mean,cren}/C_{mean,solid}$ with scaled distance from fence at the four sensor positions.

Richardson numbers of Ri = 0, 2 and 10, but excluding the case $h = 3.8$ m, Ri = 0. The layout of each of these figures is the same as those of Figs. 3–8 for the solid fence/no fence comparison of Section 3.

Comparing the crenellated fence with the solid fence, as opposed to the solid fence versus no fence as in Section 3, the C_{max} ratio is of the order of unity for the sensors upwind of the fence, irrespective of fence height for Ri > 2. In the neutral stability case there is some evidence that the C_{max} ratio increases with fence height, reaching half an order of magnitude for the highest fence considered, particularly at ground level. Dose and C_{mean}, which are otherwise similar to C_{max}, exhibit a characteristic dip at Ri = 10. This feature is also observed in the upwind plots, especially those for C_{max} and C_{mean}. The dips occur at approximately 4 fence heights upwind and approximately 12 fence heights downwind, corresponding again to the flow retardation region and the flow reattachment region, respectively, as noted in the previous section.

The time-based cloud parameter plots fail to show any marked features except an enhanced sensitivity to Richardson number at approximately 12 fence heights downwind. The time ratios as a whole are slightly less than unity, showing reduced cloud arrival and departure times when compared with those for solid fences. There is no
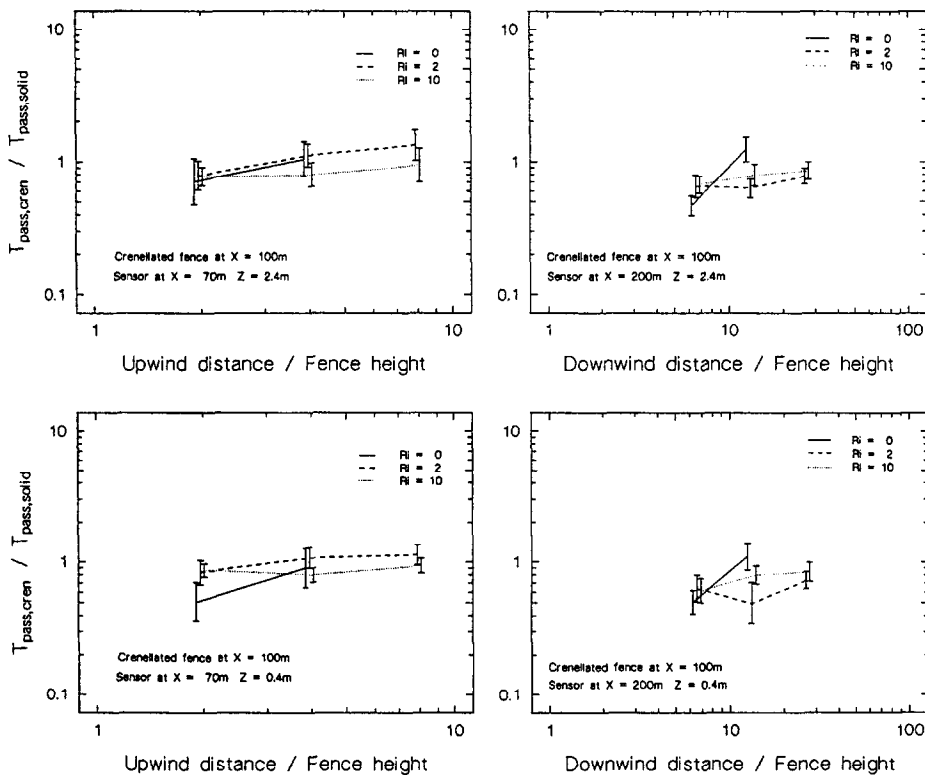

Fig. 12. Variation of $T_{pass,cren} / T_{pass,solid}$ with scaled distance from fence at the four sensor positions.
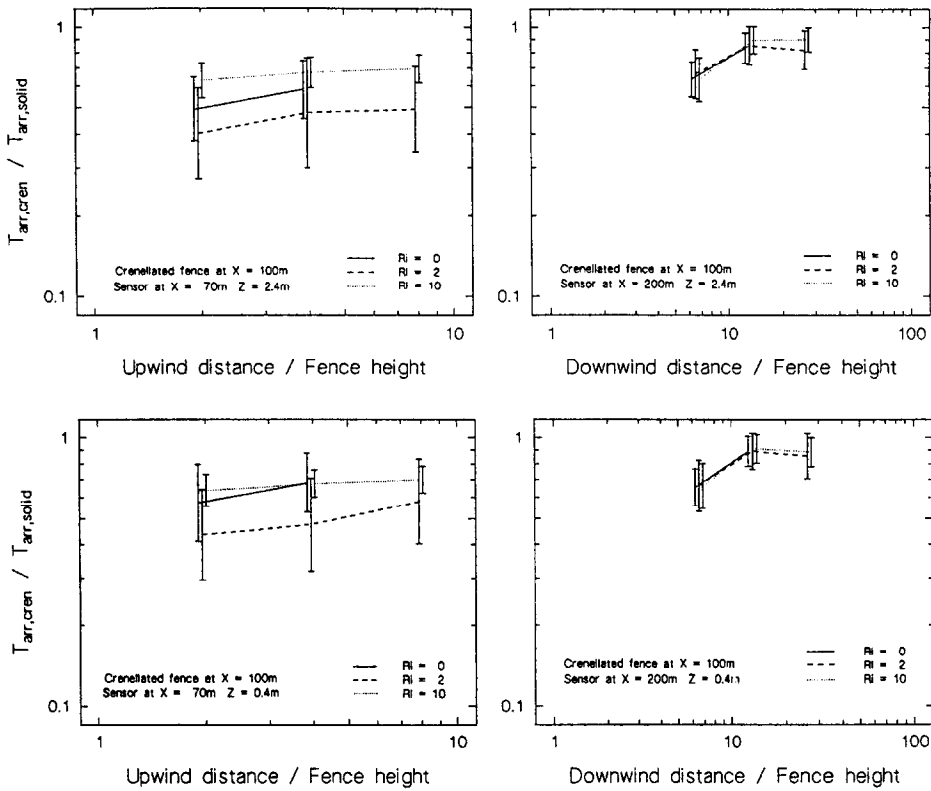
Fig. 13. Variation of $T_{arr,cren} / T_{arr,solid}$ with scaled distance from fence at the four sensor positions.

monotonic dependence on Richardson number, but rather a reversal of behaviour at $Ri = 2$, as was the case with the solid fence/no fence comparisons of Section 3.

The behaviour of the between-release variability of the crenellated fence/solid fence ratio is exemplified in the plots of C_{max} in Fig. 9. The level of variability is similar to that noted in Section 3: the minimum value of the standard deviation of the log ratio was 0.19 for the ground level sensor upwind of the fence with a fence height of 7.6 m and $Ri = 10$, and the maximum was 1.56 for the upwind sensor at $Z = 2.4$ m with a fence

Table 3
The median of the standard deviation of the log C_{max} ratio for the crenellated fence/solid fence comparison, taken over all fence height/Richardson number combinations in each quadrant. The entry in parenthese is the corresponding 90th to 10th percentile ratio

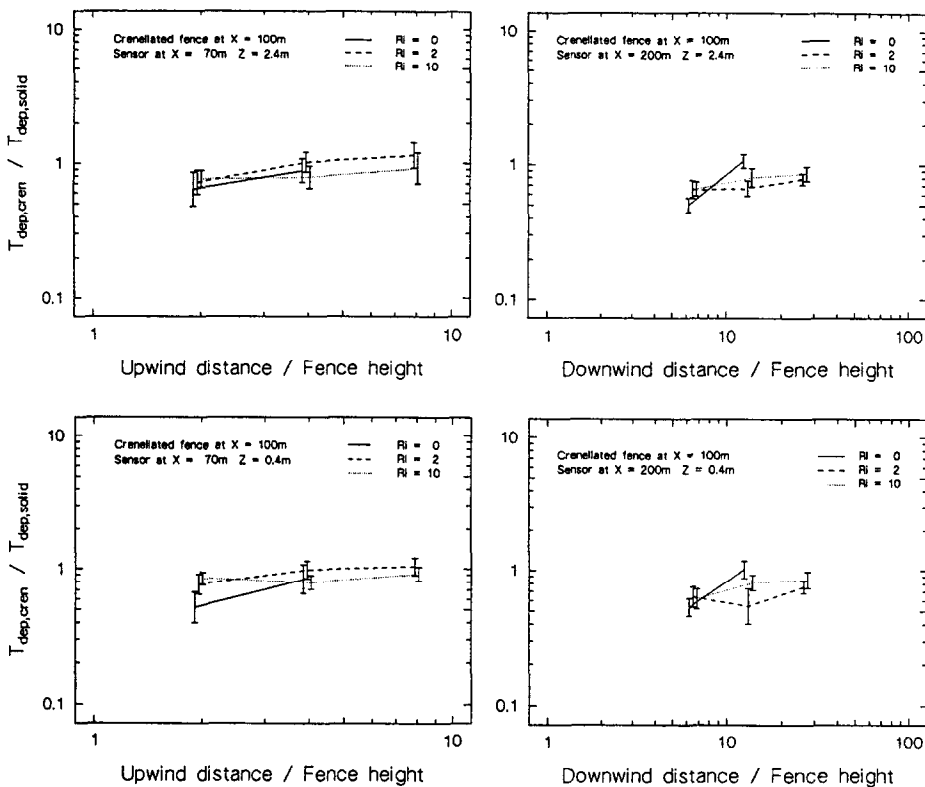|	$X = 70$ m	$X = 200$ m
$Z = 2.4$ m	0.46 (3.2:1)	0.31 (2.2:1)
$Z = 0.4$ m	0.38 (2.6:1)	0.28 (2.0:1)

Fig. 14. Variation of $T_{dep,cren} / T_{dep,solid}$ with scaled distance from fence at the four sensor positions.

height of 15.3 m and Ri = 0. The general level of variability is shown in Table 3. As before, the ratio of the 90th to the 10th percentile of $C_{max,cren}/C_{max,solid}$ is 2.0:1 for the ground level sensor downwind of the fence.

5. Summary and conclusions

As the plots discussed in Section 3 show, the effect of the interposition of a solid fence on the downwind dispersion of a heavy gas cloud from an instantaneous release is very complex. The plots demonstrate quite convincingly the presence of blocking of the passage of the gas cloud due to the fence, and also the behaviour of the cloud parameters as the upwind and downwind sensors enter the flow retardation and flow separation regions, respectively, as the fence height is increased.

From the point of view of quantitative risk assessment, however, perhaps the most interesting result to emerge is that at the downwind sampling station there was a power-law relationship between the reduction of the concentration in the gas cloud due to the presence of the solid fence and the fence height for each of the Richardson

numbers considered. It is also noteworthy that this occurs even with the lowest fence heights, where the sampling station is up to 100 fence heights downwind, for high Richardson numbers. The time-based parameters show a similar kind of behaviour, although in their case there is a consistent increase in values as the fence is approached from downwind.

The crenellated fence/solid fence comparison plots discussed in Section 4 also demonstrate the existence of blocking and flow field effects due to the fence. In this case, however, the effect of increasing the fence height is to amplify the concentration-based cloud parameters and diminish the time-based parameters. As for the solid fence/no fence comparison, the effects persist well into the far field, though it is difficult to judge the extent because of the relative sparsity of the data.

Between-release variation appears to be more prominent on the whole for the sensors upwind of the fence, particularly for the sensor at $Z = 2.4$ m. The median value of the 90th to 10th percentile C_{max} ratio, taken over all available fence height/Richardson number combinations for this sensor, is $\approx 3:1$, and an excursion of 50:1 was observed for the highest fence under neutral conditions. For the other three sensors the median C_{max} ratio is $\approx 2:1$. The reason is probably that the upwind sensor is close to the upper edge of the gas cloud in many of the test conditions, so that small variations in the depth of the gas cloud produce relatively high levels of variability.

The results concerning the mean-value behaviour of cloud parameters discussed here, derived as they are from an extensive series of replicated wind tunnel experiments, are not by themselves sufficient to enable semi-empirical modifications to be made to dense gas dispersion codes restricted to dispersion over flat terrain. However, they do provide invaluable data for the development of such codes as those incorporated into the HSE risk assessment tool RISKAT [1]. The variability data, on the other hand, could be applied in an essentially data-empirical way to provide estimates of chosen high-order percentiles of cloud parameters when computing, for example, individual risk contours even for flat terrain dispersion codes, as these results are beyond the capability of any currently available dispersion code to predict.

6. Notation

H	height of tent (m)
h	height of fence (m)
Ri	bulk Richardson number (–)
g	gravitational acceleration (m s^{-2})
ρ_{gas}	gas density of gas (kg m^{-3})
ρ_{air}	density of air (kg m^{-3})
L	characteristic length scale, $= H$ (m)
U	windspeed at height H (m s^{-1})
σ	standard deviation
n	sample size
x	downwind distance from source (m)
Z	height above ground (m)

C_{max} maximum concentration by volume of source (%)

T_{arr} dimensionless arrival time of dense gas cloud (–)

T_{dep} dimensionless departure time of dense gas cloud (–)

T_{pass} dimensionless passage time of dense gas cloud, $= T_{dep} - T_{arr}$ (–)

C_{mean} mean concentration by volume of source evaluated over the dimensionless passage time (–)

dose   concentration by volume of source integrated over the dimensionless passage time (–)

6.1. Subscripts

fence   measurement taken with solid fence in position

no fence   measurement taken over flat terrain with no fence in position

solid   see "fence" above

cren   measurement taken with crenellated fence in position

Acknowledgements

References

[1] N.W. Hurst, C. Nussey and R.P. Pape, Chem. Eng. Res. Des., 67 (1989) 362.

[2] D.J. Hall, R.A. Waters, G.A. Marsland and S.L. Upton, Repeat variability in instantaneously released gas clouds-some wind tunnel model experiments, Warren Spring Lab. Rep., No. LR 804 (PA), 1991.

[3] D.J. Hall, V. Kukadia, S.L. Upton, G.A. Marsland and M.A. Emmott, Repeat variability in instantaneously released heavy gas clouds dispersing over fences—some wind tunnel model experiments, Warren Spring Lab. Rep., No. LR 805 (PA), 1991.

[4] P.J.H. Builtjes, Research on continuous and instantaneous heavy gas clouds, Final Summary Report, TNO-IMET, Report Ref. No. 92-135, Apeldoorn, The Netherlands, 1992.

[5] J. McQuaid and B. Roebuck, Large scale field trials on dense vapour dispersion, Final Report to sponsors on the heavy gas trials at Thorney Island, 1982–1984, Commission of the European Communities, Luxembourg, Nuclear Science and Technology Report EUR 10029, 1985.

[6] A.A. Sveshnikov, Problems in Probability Theory, Mathematical Statistics and Theory of Random Functions, Dover, 1968, p. 286 and p. 461.

[7] P.W.M. Brighton, S.J. Jones, D. Martin, D.M. Webber and T. Wren, The effects of natural and man-made obstacles on heavy gas dispersion, Safety and Reliability Directorate, Reports Nos. SRD/CEC/22938/00, SRD/CEC/22938/01 and SRD/CEC/22938/02, 1991.

[8] J. McQuaid, J Hazard. Mater., 11 (1995) 1.